Structure, morphology and corrosion resistance of Zn-Ni-TiO_2 composite coatings

D. BLEJAN, D. BOGDAN[a], M. POP[b], A. V. POP[a,*], L. M. MURESAN
Department of Physical Chemistry "Babes-Bolyai" University, M. Kogalniceanu St.1, 400084 Cluj-Napoca, Romania
[a]Department of Physics, "Babes-Bolyai" University, M. Kogalniceanu St.1, 400084 Cluj-Napoca, Romania
[b] Technical University Cluj-Napoca, Faculty of Materials Science and Engineering, Department of Materials Engineering Processing, Technical University, 400641Cluj-Napoca, Romania

Composite Zn-Ni-TiO_2 layers were electrodeposited on steel, from a commercial electrolyte containing suspended TiO_2 nanoparticles. Structure, morphology and chemical composition of the Zn-Ni films were studied by XRD and SEM-EDAX methods, and corrosion resistance was evaluated by electrochemical measurements. The influence of TiO_2 nanoparticles concentration in the electrodeposition bath on the structural, morphological and corrosion properties is discussed.

(Received December 6, 2010; accepted January 26, 2011)

Keywords: Corrosion, Electrodeposition, Zinc-Nickel alloy, Zn-Ni-TiO_2 composites

1. Introduction

Although pure zinc coatings continue to be used widely for the protection of steel from corrosion, considerable efforts are being made to improve their corrosion resistance for use in harsher environment, [1,2]. One of the ways to increase the corrosion resistance of zinc coatings consists in alloying with Fe, Co, Ni. It was reported that Zn coatings containing up to 12% Ni provide cathodic protection to steel, exhibiting significantly higher corrosion resistance than pure zinc [3,4]. The corrosion resistance of Zn–Ni coatings can be further improved by the chromating treatment.

The higher corrosion resistance of the Zn–Ni coatings are strongly connected to the presence of γ-Ni_5Zn_{21} phase [5,6]. Dynamical analyses also suggest that the γ-phase is the most stable phase among all phases in Zn–Ni binary system [7].

Zinc-nickel alloy can be plated from acid or alkaline noncyanide solutions. In general, the acid bath exhibits higher cathode current efficiency but has poor deposit distribution on the substrate. Alkaline processes tend to have lower cathode current efficiency, contain complexes that affect waste treatment, but exhibit very good plate distribution [8].

An alternate process for enhancing the corrosion resistance of zinc coatings on steel consists in zinc composite coating on its surface by electrolysis of plating solutions, in which sub-micron or nano size particles (*i.e.* TiO_2, SiO_2, Al_2O_3 etc.) are suspended [9,10]. Their incorporation in the coating Ni-Zn refine the crystal size and enhances corrosion resistance, microhardness and wear resistance property. According to Brenner [11], the electrodeposition of Zn-Ni alloys occurs anomalously, (reduction of the less noble zinc is preferential), either due to a hydroxide suppression mechanism (the discharge of more noble ions is hindered by the formation of $Zn(OH)_2$ due to local pH rise) [12], or to the fact that the initial adsorbed layer of zinc inhibits the nucleation and growth of nickel nucleus [13].

In this context we analysed the combined effect of Ni and TiO_2 nanoparticles on the corrosion resistance of zinc coatings.

Zn-Ni and Zn-Ni-TiO_2 coatings were obtained by electrodeposition from a commercial alkaline bath PERFORMA 280.5 (COVENTYA SAS) containing suspended TiO_2 nanoparticles. X-ray diffraction (XRD), Scanning Electron Microscopy (SEM) and EDAX were used for determination the structure of the deposits, morphologic analysis of the surface and chemical composition. Polarization measurements were carried out in order to characterize the corrosion behavior of the coatings by using Tafel method.

2. Experimental

Zn-Ni alloys were deposited from alkaline electrolytes (pH 13) containing 82.6 g/l NaOH (Merck, Germany), 106 g/l ZINCATE 75 (containing 75g/l Zn and 400 g/l NaOH), 12mL PERFORMA 285 NI-CPL, 100mL PERFORMA 285 Base, 2 mL PERFORMA Universal and 0.7mL PERFORMA Additive K. TiO_2 nanoparticles (99.5%, 21 nm, Degussa) were added into the plating bath in order to obtain composite Zn-Ni coatings. After preparation, the electrolyte was analyzed by atomic absorbtion spectrometry, finding a Zn content 0.795g/L and Ni content of 1.392g/L. The concentrations x of TiO_2

nanoparticles were x =0 (sample S_0), x = 3 g L^{-1} (sample S_3), x = 5 g L^{-1}(sample S_5) and x=10 g L^{-1}(sample S_{10}), respectively.

Experiments were carried out in a two compartments glass cell, with the capacity of 250 ml, under magnetic stirring. The working electrode was a steel (OL37) disk electrode, (S = 0.785 cm^2). The $Ag/AgCl/KCl_{sat}$ was used as reference electrode and a Pt foil as counter electrode. The working electrode was wet polished on emery paper of different granulation and finally on felt with a suspension of alumina. Then, the electrode was ultrasonicated during 2 minutes, washed with acetone and distilled water in order to remove the impurities from the surface. For corrosion studies, a solution of 0.2 g L^{-1} $(Na)_2SO_4$ (Riedel–de Haën, Germany) (pH 5) was used. Electrochemical measurements (open circuit potential and polarization curves) were carried out using a PC-controlled potentiostat PARSTAT 2273 (Princeton Applied Research, USA). Before the polarization measurements, the open circuit potential (ocp) was recorded during 1 hour, until it was stabilized. The scan rate was 0.166 mV s^{-1}, and the sweep direction was from cathodic to anodic region. Corrosion tests were conducted at room temperature.

The deposit morphology was determined with a scanning electron microscope (SEM) (Philips XL-30). The chemical composition of the nanocomposite films was determined by using an EDAX NEW XL30 (Philips) X-ray dispersive energy analyzer attached to the SEM. The deposit structure and the preferred orientation of crystallites were determined by X-ray diffraction (XRD) analysis, using a Brucker X-ray diffractometer with a Cu K_α (λ = 0.15406 nm) at 45 kV and 40 mA. The 2θ range of 20–100º was recorded at the rate of 0.02º and 2θ /0.5 s

3. Results and discussion

Fig. 1 shows XRD pattern for four Zn-Ni coatings samples.The diffraction peaks for all samples show only the presence of γ-Ni_5Zn_{21} phase. XRD results are in agreement with as previously reported for Zn-Ni alloys [14 ,15].

The absence of TiO_2 peaks suggests that the concentration of phases associated with TiO_2 is under the limit of detection for XRD method, or their dimensions are very small on the nanoscale size.

The intensity of (hkl) XRD peaks is proportional to the density of lattice planes. Accordingly, the packing density decreased in the sequence: ρ (110) > ρ (100), [16]. The change of the grain orientations in presence of TiO_2 nanoparticles is indicated by changes of peak intensities. The intensity ratio $r = I_{(330)}/(I_{(330)}+I_{(600)})$ is dependent on TiO_2 content (Table 1).

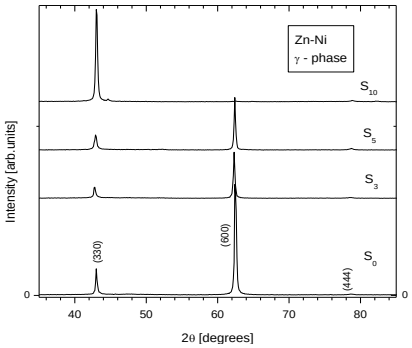

Fig. 1. XRD of S_0 coating (in the absence of TiO_2 nanoparticles, x=0) and samples S_3, S_5 and S_{10}.

The change of intensity for the diffraction peaks (330) (or (110)), and (100) (or (600)) shows textural modifications of coatings.

The increase of TiO_2 nanoparticles concentration induces an increase of the packing density associated to more closely packed (330) (or (110)) planes.

Table 1. Data obtained from XRD and EDAX.

Sample	$\frac{I(330)}{I(330)+I(600)}$ %	D [nm]	Ni wt.%
S_0 (x=0 g/l TiO_2)	13	57	16.0
S_3 (x=3 g/l TiO_2)	23	39	16.1
S_5 (x=5 g/l TiO_2)	30	30	16.5
S_{10} (x=10 g/lTiO_2)	99	44	17.0

The XRD pattern of sample S_{10} is similar with the result reported for pure γ- Ni_5Zn_{21} phase deposits obtained from alkaline solutions [17]. Crystallite sizes were determined using the Scherer formula. For all coatings, the profile of (110) peak exhibits Lorentzian line shape, as it is showed in Fig. 2.

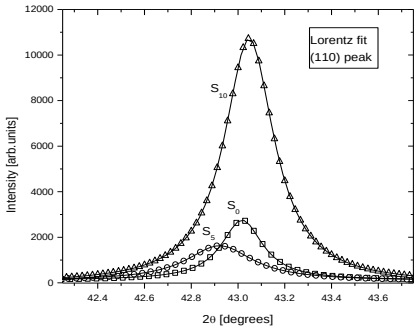

Fig. 2. The profile of (110) peak of Zn-Ni coating. The smooth curve shows the Lorentz fit of data.

Fig. 3 shows the scanning electron micrographs of Zn–Ni deposits with different TiO_2 concentration.

The grain sizes decrease from 57 nm to 30 nm with increasing TiO_2 nanoparticles concentration from zero up to 5g/l , and slowly increases for x =10 g/l, (see Table 1). The morphology of the electrodeposits varied from a fine granular shape (sample S_0, x=0.0) to a plate-like shape (sample S_5, x=5.0). Cracks are seen on the surface in the case of sample S_{10} (x=10.0). The correlation between texture and surface morphology can only be observed for large grains. The microstructural variations can be correlated with changes in the preferred crystallographic orientation. Specifically, fine granular shape corresponds to a (600) (or (100)) texture, while platelet-type grains are closely related to the (330) (or (100)) planes.

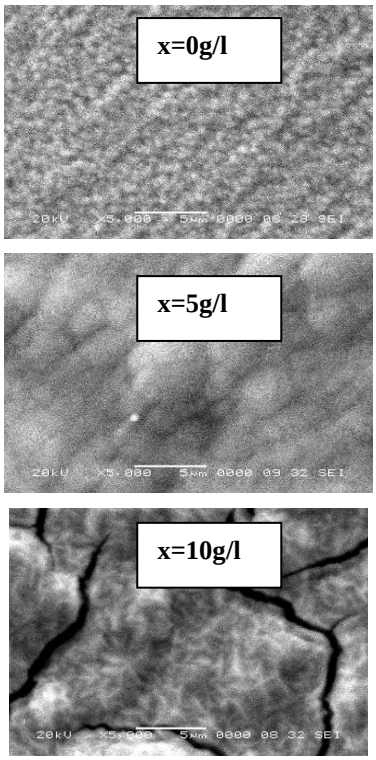

Fig. 3. SEM micrographs of the Zn–Ni deposits, showing the change of morphology with TiO_2 nanoparticle concentration.

A pyramidal microstructure coincided with a preferential (600) plane orientation was already reported [18].

The EDAX analysis (Fig. 4) shows that the Ni content increases from 16% to 17% with increasing TiO_2 concentration in bath. Similar results were obtained for Ni–Zn alloy coatings on Fe substrates [19].

The open-circuit potentials (*ocp*) for Zn-Ni and Zn-Ni-TiO_2 electrodes recorded after 1 hour of their immersion in Na_2SO_4 solution (pH 5) is presented in Table 2. In the presence of TiO_2, the *ocp* is shifted towards more positive values (Table 2) suggesting an ennoblement of the deposit, equivalent to a braking of anodic corrosion process. Differences between the values obtained for electrodes made from solutions containing 5g/L TiO_2 and 10 g/L TiO_2 is due, probably, to different amount of incorporated TiO_2 or to different roughness of the deposit.

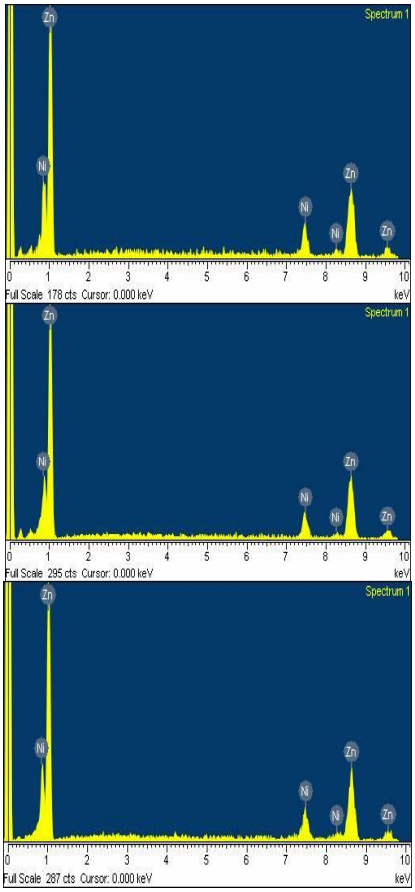

Fig. 4. EDAX analysis of Zn-Ni coatings samples S_0, S_5 and S_{10}.

Table 2. The open circuit potentials for Zn-Ni coatings after immersion in 0.2 g/l Na_2SO_4 (pH 5).

Electrode	R_p (Ω)	R/N
Zn-Ni	2523	0.998/47
Zn-Ni + TiO_2 3g/L	2662	0.998/36
Zn-Ni + TiO_2 5g/L	2893	0.999/55
Zn-Ni + TiO_2 10g/L	2192	0.998/48

Fig. 5 shows the polarization curves in a potential range of ± 20 mV.

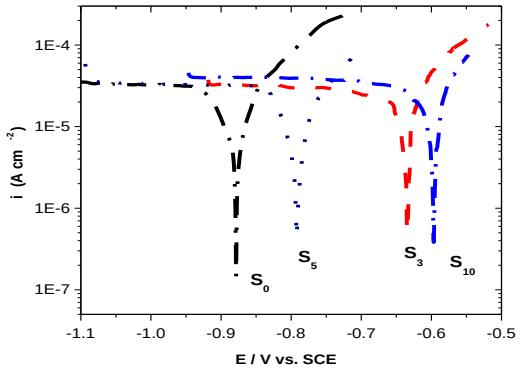

Fig. 5. Polarization curves for the Zn-Ni coated steel (samples S_0 to S_{10}).

The polarization resistance, R_p, is obtained as the inverse slope of polarization curves (Table 3).

The values of the corrosion parameters E_{cor}, i_{cor} of the coatings calculated from the polarization curves by using the Stern - Geary theory [20], are presented in Table 4.

The i_{corr} values were calculated using (β_a și β_c) anodic and cathodic activation coefficients (Tafel constants) and the polarization resistance, R_p using Stern-Geary relation [20]:

$$i_{corr} = \frac{\beta_a \beta_c}{2.3 R_p (\beta_a + \beta_c)} \quad (1)$$

Table 3. Polarisation resistance R_p values for different Zn-Ni coatings.

Sample	Electrode	ocp V *vs.* Ag/AgCl
S_0	Zn-Ni	- 0.96
S_3	Zn-Ni + TiO_2 3g/L	- 0.82
S_5	Zn-Ni + TiO_2 5g/L	- 0.87
S_{10}	Zn-Ni + TiO_2 10g/L	- 0.77

With increasing TiO_2 concentration, there is a shift of E_{corr} potential to more positive values (Table 4). There is no significant change of corrosion current intensity when TiO_2 nanoparticles were used in the plating bath.

Table 4. Kinetic parameters of the corrosion process.

Conc. TiO_2 (g/l)	E_{cor} (V)	i_{cor} (A/cm^2)	β_a (V^{-1})	$-\beta_c$ (V^{-1})
0	-0.880	7×10^{-5}	9.064	1.86
3	-0.637	6×10^{-5}	6.20	3.82
5	-0.792	2×10^{-5}	15.18	13.10
10	-0.598	4×10^{-5}	20.19	3.77

A decreasing trend of corrosion current intensity can be noticed. Best results were obtained in the deposition bath with 5g/L TiO_2 concentration. This behavior could be explained by the balance of two opposite effects. The embedded inert oxide particles diminish the surface in contact with the corrosive environment and in addition disturb the electrocrystallization process, by generating defects in the metallic matrix, which act as chemical heterogeneities and favor the corrosion process.

4. Conclusions

The XRD spectra of the Zn-Ni-TiO_2 composite coatings shows the characteristic diffraction pattern only for γ-Ni_5Zn_{21} phase. This phase is responsible for the good corrosion resistance a of Zn–Ni coatings.

A correlation between preferred crystallographic orientation and surface morphology of the electrodeposits was evidenced. Fine granular shape corresponds to a (600) (or (100)) texture, while platelet type grains are closely related to the (330) (or (100)) component The addition of TiO_2 in Zn-Ni improve little the corrosion resistance. The influence of TiO_2 nanoparticles on corrosion behavior can be explained by decreasing the contact surface with corrosive environment but in the same time generating defects in metallic matrix.

Acknowledgment

One of the authors (D. Blejan) gratefully acknowledge the financial support within the POSDU /88/1.5/S/60185 Babeș-Bolyai University, Cluj-Napoca, Romania

References

[1] V. G. Roev, R. A. Kaidrikov, A. B. Khakimullin, Russian Journal of Electrochemistry, **37**(7), 756 (2001).
[2] Hwa Young Lee, Sung Gyu Kim, Surf. and Coat. Technol. **135**, 69 (2000).
[3] O. Hammami, L. Dhouibi, E. Triki, Surf. Coat. Technol., 2863 (2008).
[4] N. Zaki, Met. Finish. **87**, 57 (1989).
[5] R. Fratesi, G. Roventi, Surf. Coat. Technol. **82**, 158 (1996)
[6] Y. F. Jiang, L. F. Liu, C. Q. Zhai, Y. P. Zhu, W. J. Ding,Thin Solid Films **484**, 232 (2005).
[7] J. T. Lu, J. H. Chen, Q. Y. Xu, G. Kong, L. X. Liu, Mater. Prot. **30**, 8 (1997).
[8] P. Ganeshan, S. P. Kumaraguru, B. N. Popov, Surf & Coat. Technol., **201**, 7896 (2007).
[9] J. Fustes, A. Gomes, M. I. da Silva Pereira, J. Solid State Electrochem, **12**, 1435 (2008).
[10] B. M. Praveen, T. V. Venkatesha, Applied Surface Science **254**, 2418 (2008).
[11] A. Brenner, Electrodeposition of Alloys, Academic Press, **1**, New York and London, 77 (1963).
[12] H. Dahms, J. Electroanal. Chem. **8**, 5 (1964); R. Valotkiene, K. Leinartkas, D. Virbalyte, E. Juzeliunas, Chemija (Vilnius), T **12**(4), 236 (2001).

[13] S. G. Y. Li, J. S. Lian, L. Y. Niu, Z. H. Jiang, Surf. Coat. Technol. **191**, 59 (2005).
[14] L. S. Tsybulskaya, T. V. Gaevskaya, O. G. Purovskaya, T. V. Byk, Surf. & Coat. Technol. **203**, 234 (2008).
[15] Metals Handbook, 9th ed., ASM International, 3 (1992).
[16] F. Mansfeld, S. Gilman, J. Electrochem. Soc. **117**, 588 (1970).
[17] M. S. Chandrasekar, S. Srinivasan, M. Pushpavanam, J. Solid State Electrochem **13**, 781 (2009).
[18] L. Felloni, R. Fratesi, E. Quadrini, G. Roventi, J. Appl. Electrochem., **17**, 574 (1987).
[19] E. Raub, F. Elser, Metalloberflache **11**(5), 165 (1957).
[20] M. Stern, A. L. Geary, J. Electrochem. Soc. **104**, 56 (1957).
[21] A. Hovestad, L. J. J. Jansen J. Appl. Electrochem. **25**, 519 (1995).

*Corresponding author: aurel.pop@phys.ubbcluj.ro